Food Sci. Technol. Int. Tokyo, **3** (3), 226–234, 1997

Review

Advances in Mathematical Modeling of Heat and Mass Transfer during Throughflow-Air Drying of Cereal Grain

Shahab SOKHANSANJ, Weiguo LANG and Deqiang GU

Department of Agricultural and Bioresource Engineering, University of Saskatchewan, 57 Campus Drive, Saskatoon Sk S7N 5A9, Canada

Received July 2, 1997; Accepted July 2, 1997

This paper discusses recent advances in cereal drying. It focuses on mathematical modeling of convective heat and mass transfer using air as the drying medium. The mathematical modeling of air distribution follows conservation of momentum and a constituent equation relatinng the velocity of air to its static pressure. The paper presents data obtained from a series of detailed wheat drying experiments. It is shown that the existing simulation models can be improved once the thin layer drying equation is updated spatially and temporally within the bulk grain. The use of variable properties in calculating transient moisture contents and temperatures also improves the accuracy of mathematical simulations.

Keywords: cereal drying, heat, mass, momentum transfer, modeling, simulation, experimental drying, airflow, bulk grain drying, throughflow drying

Drying of agricultural grains for safe storage has been practiced for centuries but major progress in modern artificial drying equipment and mathematical simulations dates back only three to four decades. Mathematical simulations have become an efficient and economical tool to aid the design of dryers and to evaluate existing drying systems for performance.

The through flow dryer is a convection system in which the drying air passes through the permeable product. The product is usually in the form of granular, stemmy or leafy solid particles. We call this type of dryer *through flow* since the drying medium (air) flows through the bed of the solids. The transfer of moisture takes place on the surface of the particles. In other types of convection drying, the drying air does not penetrate into the bed of the solids.

Approaches to model development in throughflow drying can be classified into three categories: empirical formulations (Boyce, 1965), semi-empirical equations (Ingram, 1976) and theoretical models based on the physics of drying (Bakker-Arkema *et al.*, 1974). Inspite of extensive simulation work for almost every major agricultural grain, a significant improvements in the basic drying equations have not taken place over the past twenty years. Recent advances in through flow modeling include two dimensional model by Arthur and Rumsey (1986), diffusion model by Nishiyama (1987) and by Fasina and Sokhansanj (1995). Research trends and opportunities in advancing the drying science for agricultural grains and forages have been discussed by Sokhansanj and Raghavan (1996).

Grains vary in hygroscopic characteristics which are prime parameters involved in the drying process, and chemical and physiological properties which also play important roles in drying. Simulating the drying process precisely is difficult, especially for deep-bed drying. Most of the deep-bed drying simulations have been based upon the assumption that a deep-bed could be regarded as a series of thin layers. Since thin layer drying could be successfully predicted, the applicability of the thin layer to deep-bed drying was implied. This assumption is questionable. In thin-layer drying, one layer of grain kernels is fully exposed to a constant inlet air. In deep-bed drying however, the inlet air conditions (temperature, humidity) passing through the bed vary continuously until it exits the bed.

The objective of this paper is to describe the most widely used mathematical models of high temperature throughflow drying for cereals and recent progress made in improving these models. Models that deal with low temperature drying of grains (drying air temperatures less than 30°C) are not dealt with in this research.

Heat and Mass Transfer Based Drying Models

In a drying system, four components participate in the process, i.e. dry grain, moisture in the grain, dry air, and vapor in the air. For a controlled volume the conservation of mass is written as:

$$\nabla\cdot(v\rho)+\frac{\partial\rho}{\partial t}=r \qquad (1)$$

where r is an exchange term for the mass transfer among components in the system. Likewise, the conservation of energy on the control volume is written as:

$$\nabla\cdot(v\rho h)+\frac{\partial}{\partial t}(\rho h)=q \qquad (2)$$

where h is the enthalpy of each component and is a scalar quantity representing sensible and latent heat contents.

The density of water vapor in the air and the density of moisture in the grain can be expressed as a mass fraction H and M in the air and in the solid, respectively:

$$\rho_v=\rho_a H \tag{3}$$

$$\rho_w=\rho_p M \tag{4}$$

The latent heat content of the solid and of the dry air is zero since there is no moisture in them. The latent heat content of the water vapor in the air is h_{fg} and that of the moisture in the product is h_{fg}'.

Enthalpy for dry air:

$$h=C_a T \tag{5}$$

and for dry solid:

$$h=C_p\theta \tag{6}$$

for the moisture in the grain:

$$h_m=C_w\theta+h_{fg}' \tag{7}$$

and for the water vapor in the air:

$$h_v=C_v T+h_{fg}. \tag{8}$$

In writing equations (5)-(8) we have assumed that enthalpy at 0°C is zero. Next step is to write equations (1) and (2) for each component of the system, replacing densities and enthalpies with definitions (3)-(8).

$$g_p\cdot\nabla M+\rho_p\frac{\partial M}{\partial t}=r_m \tag{9}$$

$$g_a\cdot\nabla H+\rho_p\frac{\partial H}{\partial t}=-r_m \tag{10}$$

$$g_p\cdot\nabla[C_p\theta+M(C_w\theta+h_{fg}')]+\rho_p\frac{\partial}{\partial t}[C_p\theta+M(C_w\theta+h_{fg}')]=q \tag{11}$$

$$g_a\cdot\nabla[C_a T+H(C_v T+h_{fg})]+\rho_a\frac{\partial}{\partial t}[C_a T+H(C_v T+h_{fg})]=-q \tag{12}$$

The major assumption in equations (9)-(12) is a constant denity. Each q is defined as total energy convectively transferred between grain and air. Since the air and vapor are assumed to be in temperature equilibrium, there is no transfer between these components and they may be combined for the purpose of heat transfer. The same applies to the grain-moisture mixture. When these terms are lumped together, we can write the equation which describes convective transfer from air-vapor mixture to moist grain.

$$q_p+q_m=-(q_a+q_v)=ha(T-\theta) \tag{14}$$

where h is the convective heat transfer coefficient and a is the specific surface area (area/volume).

Equations (9)-(12) take up the following form in a one dimensional drying system:

$$g_p\frac{\partial M}{\partial x}+\rho_p\frac{\partial M}{\partial t}=r_m \tag{15}$$

$$g_a\frac{\partial H}{\partial x}+\rho_p\frac{\partial H}{\partial t}=-r_m \tag{16}$$

$$g_p\frac{\partial}{\partial x}[C_p\theta+M(C_w\theta+h_{fg}')]+\rho_p\frac{\partial}{\partial t}[C_p\theta+M(C_w\theta+h_{fg}')]=ha(T-\theta) \tag{17}$$

$$g_a\frac{\partial}{\partial x}([C_a T+H(C_v T+h_{fg})]+\rho_a\frac{\partial}{\partial t}[C_a T+H(C_v T+h_{fg})]=-ha(T-\theta) \tag{18}$$

Equations (15)-(18) describe the convective heat and mass transfer between grain and air. Diffusive heat and mass transfer equations are added to these system if internal temperature and moisture of grain are to be calculated.

Equations (15)-(18) can be simplified further for a variety of drying situations and drying configurations. For instance in a fixed bed dryer $g_p=0$ because the grain is stationary.

$$\rho_p\frac{\partial M}{\partial t}=r_m \tag{19}$$

$$g_a\frac{\partial H}{\partial x}+\rho_a\frac{\partial H}{\partial t}=-r_m \tag{20}$$

$$\rho_p\frac{\partial}{\partial t}[C_p\theta+M(C_w\theta+h_{fg}')]=ha(T-\theta) \tag{21}$$

$$g_a\frac{\partial}{\partial x}[C_a T+H(C_v T+h_{fg})]+\rho_a\frac{\partial}{\partial t}[C_a T+H(C_v T+h_{fg})]=-ha(T-\theta) \tag{22}$$

Researchers and engineers have adapted equations (19)-(22) for a variety of dryer configuration. The Bakker-Arkema drying model (Bakker-Arkema *et al.*, 1974) is a simplification of eqations (19)-(22) as follows:

$$\frac{\partial M}{\partial t}=k(M-M_e) \tag{23}$$

$$\frac{\partial H}{\partial x}=-\frac{\rho_p}{g_a}\frac{\partial M}{\partial t} \tag{24}$$

$$\frac{\partial\theta}{\partial t}=\frac{ha}{\rho_p C_p+\rho_p C_w M}(T-\theta)+\frac{h_{fg}+C_v(T-\theta)}{\rho_p C_p+\rho_p C_w M}g_a\frac{\partial H}{\partial x} \tag{25}$$

$$\frac{\partial T}{\partial x}=\frac{-ha}{g_a C_a+g_a C_v H}(T-\theta) \tag{26}$$

The assumptions inherent in these equations are: (1) terms associated with transient air temperatures and transient humidity ratio are negligible because both of these terms are small compared to the temperature and humidity ratio gradients (variation with x); (2) the heat of adsorption and desorption are lumped in h_{fg} in equation (25). Although assumption (1) seems reasonable, the impact of assumption (2) on the solution accuracy must be analyzed. Further assumptions are: negligible shrinkage, no heat and mass losses from the system, and parallel airflow pattern, constant parameters during a short time period and a thin layer equation similar to (23) to represent the instantaneous drying rate of a fully exposed grain.

Numerical Solutions of Drying Model

A forward numerical scheme was used to solve simulataneously the four equations (23)-(26).

$$T_{x+\Delta x,t}=\frac{-ha}{g_a C_a+g_a C_v H_{x,t}}(T_{x,t}-\theta_{x,t})\Delta x+T_{x,t} \tag{27}$$

$$\theta_{t+\Delta t,x}=\frac{ha(T_{x,t}-\theta_{x,t})+\left[h_{fg}+C_v(T_{x,t}-\theta_{x,t})g_a\frac{\Delta H}{\Delta x}\right]}{\rho_p C_p+\rho_p C_w M_{x,t}}\times\Delta t+\theta_{x,t} \tag{28}$$

$$H_{x+\Delta x,t}=-\frac{\rho_p}{g_a}\frac{\Delta M}{\Delta t}\Delta x+H_{x,t} \tag{29}$$

$$M_{x,t+\Delta t}=[k(M_{x,t}-M_e)]\Delta t+M_{x,t} \tag{30}$$

Equations (27)-(30) require numerical values for h, a, C, ρ_p, ρ_a, M_e, and k. Lang (1993) established the following

values for simulating the drying of wheat in a fixed bed dryer.

Density Bulk density equations derived from experimental moisture desorption tests (Lang, 1994) as follows:

$$\rho_b = 760[1 - 0.44M + 0.1963M^2] \quad (31)$$

where M is percennt dry basis moisture content.

Drying constant The moisture ratio equation was given by:

$$MR = \frac{M - M_e}{M_i - M_e} = \exp[-kt] \quad (32)$$

where M is percent dry basis moisture content. For wheat, k was given by O'Callaghan *et al.* (1971):

$$k = 2000\exp\left[\frac{-5094}{T + 273}\right] \quad (33)$$

where T is in °C. The unit of k in equations (32) and (33) is in s^{-1}.

Equilibrium moisture content For wheat, the equilibrium moisture content model presented by O'Callaghan *et al.* (1971) is used:

$$M_e = \left[\frac{\sqrt{H}}{(1.8T + 32)^2}\right]^{1/1.57} + 0.0615 \quad (34)$$

where H is the humidity ratio of the air, decimal and T is the air temperature, °C. M_e is equilibrium moisture content (decimal dry basis).

Latent heat of evaporation The latent heat of evaporation of free water can be found from thermodynamic tables as 2,250 kJ/kg. The total latent heat of evaporation for grains can be found by:

$$h'_{fg} = h_{fg}[1 + a\exp(-bM)] \quad (35)$$

where a and b are constants varying from grain to grain. For wheat, $a=23$ and $b=40$ and M is decimal dry basis.

Specific heat For wheat, the specific heat was calculated using Muir and Viravanichai (1972) formula:

$$C_p = 1.14 + 3.91M \quad (36)$$

where M is moisture content of grain on a decimal dry basis. The units of C_p in equation (36) are in kJ $kg^{-1}K^{-1}$.

Convective heat transfer coefficient The heat transfer coefficient for grain was not readily available in the literature, but it could be calculated from the Nusselt number. The volumetric convective heat transfer coefficient of wheat was taken from Boyce (1965) as a function of the air mass flow rate, g_a, the air temperature, T, and atmospheric pressure, P_{atm}:

$$h_v = 8.6\times10^8\left[\frac{g_a(T + 273)}{P_{atm}}\right]^{0.6} \quad (37)$$

Improvements to the Simulation Model

Time factor One of the factors causing inaccuracy of grain drying simulation was related to assignment of drying conditions to the first layer of the grain in the bed. Normally, the air conditions of the first layer were assigned to be equal to the inlet air conditions at the beginning of each new time interval. This simulation method could cause errors because air in the first layer may not be the same as the inlet air during the initial period because a large instantaneous heat and mass transfer is involved at this location. Therefore, a time factor was considered. From experimental data of temperatures and moisture contents during drying, an exponential form of a time factor was developed by trial and error as follows:

$$f_t = 1 - \exp(-t/\tau) \quad (38)$$

where f_t is the time factor, and τ is the time constant (1/s) estimated as follows:

$$\tau = 110(1 - 0.010T) \quad (39)$$

where T is in °C. As the drying proceeds, the first layer grain dries and the drying air in the first layer approaches the inlet air conditions. The time factor approaches unity. Air temperature and humidity assigned to the first layer were multiplied by the time factor.

Layer factor In thin-layer, grain kernels are exposed fully to the inlet drying air. In the case of deep-bed drying, however, the bottom of a layer within the bed is exposed to the exhausted air from the lower layer, and the top of the layer is in contact with the bottom of the upper layer. We have a clear evidence that simulated drying conditions for a few layer close to the air entry into a bed agrees well with the experimental data. But disagreement between experimental data and simulated data propagates with distance from the air entry. A layer factor, therefore, should be considered to compensate for the deviation from an ideal thin layer situation:

$$f_x = \exp(-\xi x/L) \quad (40)$$

where f_x is the layer factor, x and L are the layer location in the bed and the thickness of the bed, respectively, m. ξ is estimated by:

$$\xi = 0.25(1 - 0.009T) \quad (41)$$

where T is in °C. For the bottom layer where $x=0$, the layer factor is equal to one. The thin layer drying equation will hold for the first layer. As drying progresses further away from the bottom, the value of the factor decreases. Modification was made to multiply the drying constants, k, in the thin layer drying equation by the layer factor, f_x.

Shrinkage computation The porosity of bulk wheat changes with moisture content during drying as follows:

$$\varepsilon = 0.10 + 0.08M - 0.54M^2 \quad (42)$$

where M is percent kernel moisture content dry basis.

A shrinkage coefficient, λ_m, was developed:

$$\frac{\partial x}{\partial M} = \lambda_m \quad (43)$$

When simulation runs were performed, a constant number of layers but variable thickness of each layer scheme was used. The scheme was so designed that the number of divided layers in the whole drying bed remained unchanged while the thickness of each layer varied with average moisture content of that layer during a time interval:

$$N = \frac{L_0}{\Delta x_0} \quad (44)$$

where N is the number of layers in the drying bed, and L_0 and ΔX_0 are the initial bed thickness and the initial divided layer thickness, respectively.

The instantaneous bed thickness, L_t, varied during drying due to shrinkage as moisture was removed. The shrinkage of a layer, i, was calculated as:

$$\delta S_i = \lambda_m \Delta M_i \quad (45)$$

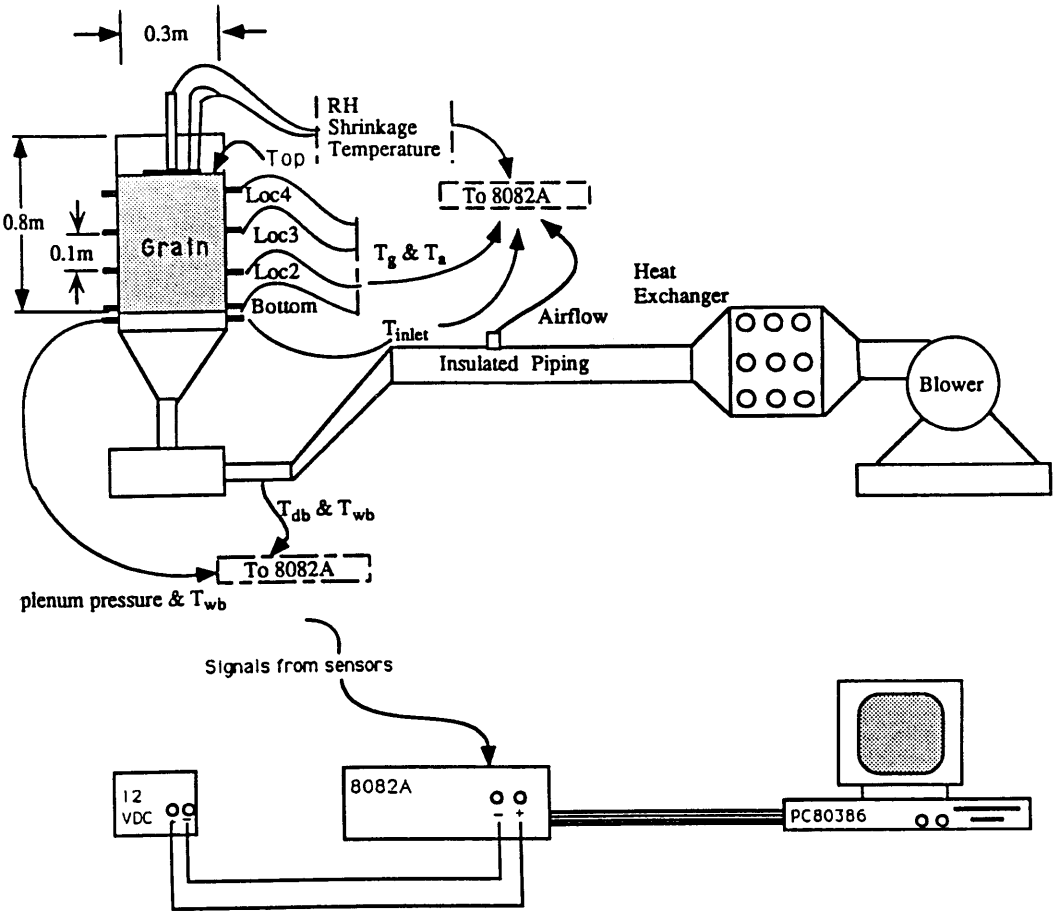

Fig. 1. Schematic diagram of the test set up for drying tests.

At the end of each time interval, the total bed shrinkage was the sum of the layer shrinkage:

$$S_t=\sum_{i=1}^{N}\delta S_i \tag{46}$$

A new instantaneous bed thickness was found by:

$$L_t=L_o-S_t \tag{47}$$

The new layer thickness was then:

$$\Delta_x=\frac{L_\theta}{N} \tag{48}$$

Before starting simulation for a new time interval, the new layer locations were first found and the old layer thickness was replaced with the new value calculated using (49):

$$\Delta x=\frac{L_o-\Sigma(\lambda_m\Delta M_x)}{N} \tag{49}$$

At the beginning of each time interval, the drying conditions for the first layer were assigned to be: $T_1=\theta_1=(T_{in}f_t)$ and $H_1=(H_{in}f_t)$ where T_{in} and H_{in} are the inlet air temperature and humidity. The air temperature and humidity ratio at $(x+\Delta x,t)$ and the grain temperature and moisture content at $(x, t+\Delta t)$ were computed from previously known values at (x,t). During the time interval, the computation was continued through the grain bed by step Δx. The simulation was completed when the moisture content reached a desired level.

Simulation and Experimental Drying Data

Lang (1993) conducted a series of experiments on the deep-bed drying of canola and wheat. Figure 1 shows the experimental set up that consisted of a cylindrical column 30 cm diameter and 80 cm high. Tobin cultivar of canola (*Brassica campestris* L) and Kenyon variety of wheat (*Triticum aestivum* L) were used. The grains were cleaned and sorted. The moisture contents of grains were reconstituted with the addition of water to obtain the desired moisture content levels.

The experimental column was filled to 40 cm high with grain. Because of different resistance of canola and wheat to airflow, the same opening at the blower inlet resulted in different airflow rates into the dryer. The frontal air velocity for wheat was higher than that for canola by about 0.1 m/s. Grain moisture content, air and grain temperatures, inlet and outlet air relative humidities, static pressure, airflow rate, and bed shrinkage during each experimental run were measured and recorded.

The drying simulations were performed for canola and wheat using equations (27)-(30) with constant properties (original model) and with improvements in drying rate and layer factors and bulk shrinkage shrinkage (modified model). The input data to the drying model were similar to the experimental condition: drying air temperature 65°C, relative humidity 10%, initial moisture content of canola 23% and that

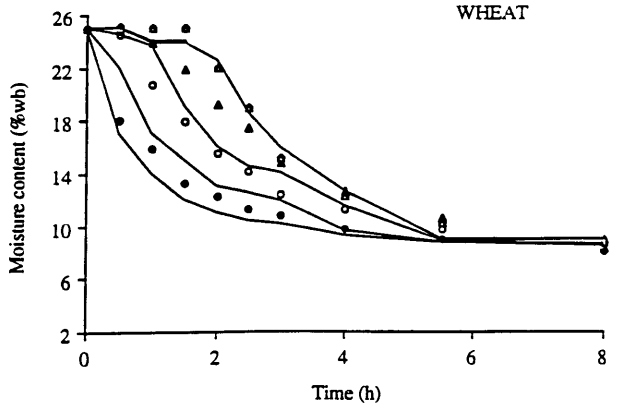

Fig. 2. Experimental and simulated moisture content using the original Bakker-Arkema's model. Wheat: ● Bottom, ○ Loc 2, ▲ Loc 3, △ Loc 4, — Predicted.

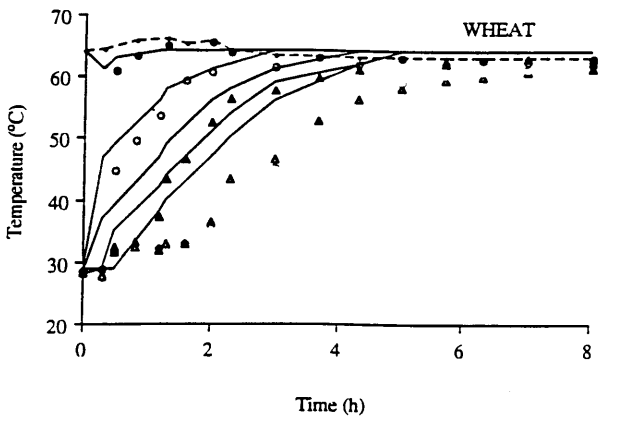

Fig. 4. Experimental and simulated temperatures using the original Bakker-Arkema's model. Wheat: ● Bottom, ○ Loc 2, ▲ Loc 3, △ Loc 4, — Predicted.

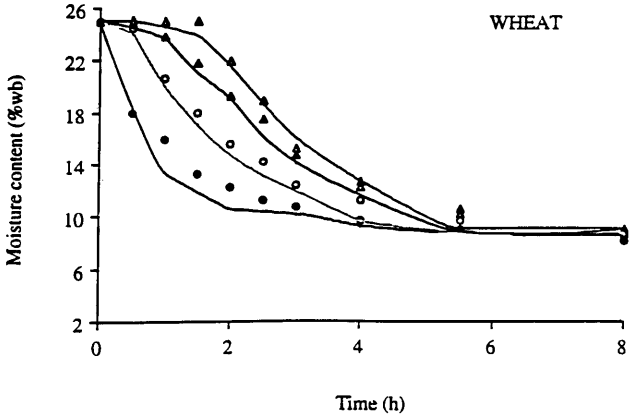

Fig. 3. Experimental and simulated moisture content using the modified Bakker-Arkema's model. Wheat: ● Bottom, ○ Loc 2, ▲ Loc 3, △ Loc 4, — Predicted.

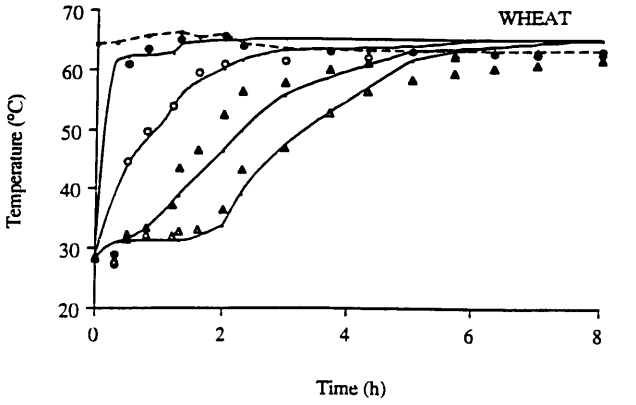

Fig. 5. Experimental and simulated temperatures using the modified Bakker-Arkema's model. Wheat: — Inlet, ● Bottom, ○ Loc 2, ▲ Loc 3, △ Loc. 4, — Predicted.

of wheat 26% (wet basis), airflow rate 0.32 m/s and 0.42 m/s for canola and wheat respectively. The results for wheat is explained in this paper. For results on canola see Lang (1993).

Moisture content Moisture contents predicted using the original and modified drying model for wheat are shown in Figs. 2 and 3. Moisture content at the bottom layer was calculated satisfactorily in both models. As the drying front moved upwards, the difference between prediction (calculated) and experiment increased. This was because, as discussed previously, the drying at the first layer was close to the situation of the thin layer drying, the drying equation worked well. Curve shapes at location 3 and the top were different from the bottom and at location 2. The modified model calculated moisture contents in the middle and at the top layer more accurately than the original model. Agreements between the experimental and simulated improved for the upper layers. Results from the simulation were faster in drying than experimental results for the lower layers. This phenomenon probably indicated that the thin layer drying constant, k, from O'Callaghan *et al.* (1971) was large when it was applied to the drying in upper layers of the bed. The large drying constant was reduced by the layer factor when the simulated drying location moved to the upper layers.

Temperature Figures 4 and 5 shows predicted temperature compared to experimental data for high temperature drying of wheat. A large difference was found for Loc 3 (20 cm from the bottom). The simulation at the bottom and Loc 2 (10 cm from the bottom) showed no cooling period. About 20-min cooling period and another 40-min heating period for the bottom layer temperature to equilibrate with the inlet air temperature were found from the experiment. These cooling and heating transition periods indicated that during the initial drying period (about 1 h) temperature in the first layer was not equal to the inlet air temperature. Thus, the time factor was necessary. In this particular case, the time factor should be further reduced.

Generally the model predicted temperatures better in a high temperature drying than in a low temperature drying, and with respect to grain type, better for wheat than for canola.

Airflow through Bulk Wheat

The size, shape, and position of air inlets to a grain bin affect the rate of drying and cooling of the grain. A flat fully perforated floor introduces uniform airflow pattern and hence

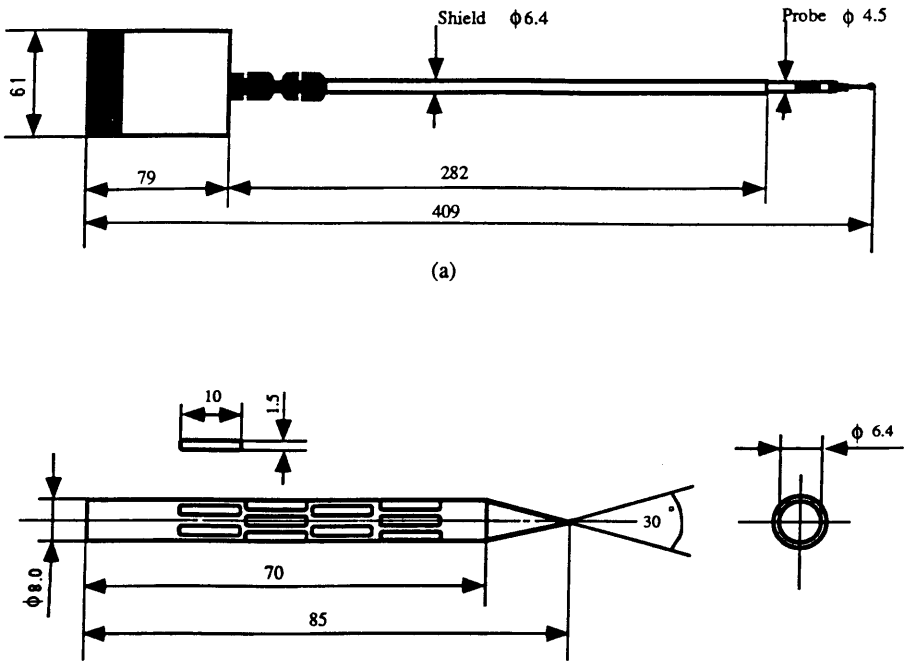

Fig. 6. Schematic diagram of the bare (a) and shielded (b) sensor for intergranular air speed measurements (dimensions in mm).

uniform drying because the air particles travel in parallel stream lines. A partially perforated or a conical shaped floor, on the other hand, introduces non parallel airflow streamline into the grain mass. A grain that is not dried or cooled uniformly is prone to spoilage.

Mathematical modeling The literature contains a number of studies on airflow distribution in grain bins either experimentally (Brooker, 1959) or mathematically (Brooker, 1961; Segerlind, 1982; Miketinac & Sokhansanj, 1985; Gu *et al.*, 1996). These studies were focused on air pressures within the grain mass. The modeling of airflow distribution in grain bins follows the mathematical procedure developed by Brooker (1961) and modified later by Segerlind (1982). A relationship in the form of:

$$V_n=A\left(\frac{\partial P}{\partial n}\right)^B \tag{50}$$

proposed by Shedd (1953) is used to relate velocity to pressure gradient. In equation (50) V_n is the air velocity approaching the grain mass (facial velocity) and $\partial p/\partial n$ is the magnitude of pressure gradient. The constants A and B are determined experimentally for each range of air velocity upon which they can be taken to be constant. Li (1992) developed the following values for clean wheat (Katepwa variety) at a moisture content of 18%:

for $V\leq 0.021$ m/s

$$A=0.646\times10^{-3},\ B=0.945 \tag{51}$$

and for $V>0.021$ m/s

$$A=1.855\times10^{-3},\ B=0.704 \tag{52}$$

For low air speeds, equation (51) satisfies Darcy's relation for flow in a porous medium. For higher flow rates, the pressure velocity relationship is nonlinear. Since the absolute temperature and pressure changes were small, incompressible steady flow was assumed and the continuity equation was written:

$$\frac{\partial V_x}{\partial x}+\frac{\partial V_y}{\partial y}=0 \tag{53}$$

By assuming a linear correspondence between pressure gradient vectors and velocity vectors, Brooker *et al.* (1974) proposed the following equations to relate the velocity components in the direction of x or y to the normal velocity:

$$V_i=\frac{\partial P/\partial i}{\partial P/\partial n}V_n \quad i=x,y \tag{54}$$

For numerical calculations, it is convenient to lineralize the relationship between the velocity vector and the pressure gradient. A granular permeability is defined as:

$$G=\frac{V_n}{\partial P/\partial n}=A\left(\frac{\partial P}{\partial n}\right)^{B-1} \tag{55}$$

Substituting equation (55) in equation (54) and (53) yields:

$$\frac{\partial}{\partial x}\left(G\frac{\partial P}{\partial x}\right)+\frac{\partial}{\partial y}\left(G\frac{\partial P}{\partial y}\right)=0 \tag{56}$$

Equation (56) is a two dimensional form of the governing differential equation of the pressure field and can be solved using an iterative numerical scheme.

The finite element computer package PC-SEEP (Lam 1990) that solves equation (56) for flow through porous soil was used to simulate airflow distributions in the grain mass. A total of 340 simplex triangular elements for configurations flat and partially perforated floors, and 446 elements for configuration conical floor were generated. At the air inlet and the top surface of the grain bed, the boundary conditions

were set as P=300 Pa and P=0 (atmospheric pressure) respectively. The wall of the bin was assumed to be impervious.

Experiments The experimental equipment consisted of a rectangular grain bin, a blower, and instrumentation. The grain bin was 1.5 m in length, 0.5 m in width. The height of the bin was either 1.5 m for the totally perforated floor and the partially perforated floor, and 1.8 m for the slanted floor. The perforations in the plank were circular holes 1 mm in diameter providing an inlet open area of about 13%. Air was supplied by a variable speed centrifugal blower through a circular duct connected to the plenum under the bin. The air flow rate was measured by a pitot tube installed in the straight section of the supply air duct.

The sensor to detect intergranular air speed was a TSI Model 8470—omni directional hot wire anemometer (TSI Inc., Minneapolis, MN). A favorable characteristic of the sensor was its small tip (ϕ=3 mm) which was close to the size of a wheat kernel (2.5 mm×2.6 mm×6 mm). The sensor's tip was extremely fragile and to prevent its direct contact with the grain surface several protective shields were designed and constructed. After extensive tests, a slotted shield made of stainless tubing (Fig. 6) was constructed. The shield was 85 mm in length and 8.0 mm in diameter with longitudinal slots yielding an open area of about 65%.

Cleaned hard red spring wheat with a moisture content of 9.8% was obtained from an experimental farm in Saskatoon. For drying test grain was remoistened to 21% by spraying water on the grain, mixing and conditioning. The grain bin was filled with the moist grain to a volume of 1.05 m^3 (±0.08 m^3) and the top surface of the grain was leveled.

The flow sensors were inserted into the grain mass horizontally through the front wall such that the sensor tip were in a vertical plane about 280 mm from the front wall. Sampling points were located evenly throughout the bin. Static pressures within the grain mass were measured with stainless steel tubes inserted horizontally halfway between two adjacent air speed sensors. The static pressure in the plenum under the bin was also measured with a tube. Moisture contents were measured using a grain sampler, drawing samples from grain mass. Temperatures were measured with thermocouples inserted into the grain mass. Ambient air temperature and relative humidity were recorded.

Drying tests were conducted with fully perforated floor, partially perforated floor and slanted perforated floor while maintaining the static pressure in the plenum constant at 300 Pa by adjusting the rotational speed of the blower. A drying test lasted five to eight days.

Calculated and experimental results Analysis of the results from the tests in the bin with fully perforated floor shows a linear relationship between the measured intergranular air velocity, V_m, and facial air velocity, V_0.

$$V_m=6.827V_0+0.056,\ R^2=0.95. \qquad (57)$$

The facial air speed V_0 was calculated from velocity pressure data published in the ASAE Standards (1996). The usual practice is to calculate intergranular air velocity from dividing the facial velocity by grain bulk porosity (Brooker *et al.*, 1992). For wheat this porosity is 0.43 or its inverse is 2.3. The slope of equation (57) suggests that inverse is 6.8. Carman (1956) attributed the higher ratio (lower porosity) to tortuosity of irregular shaped particles with random packing. Garrett and Brooker (1965) analyzed the aerodynamic properties of a single seed and suggested that for agricultural grains the ratio of V_m/V_0 is between 2.3 and 10.7. The ratio 6.827 obtained from our tests falls in the range specified by Garrett and Brooker (1965).

Figure 7 shows the typical measured and the simulated (in brackets) air speeds at each sampling points in the bin with slanted floor. The speeds marked as ">0.5" indicate that the

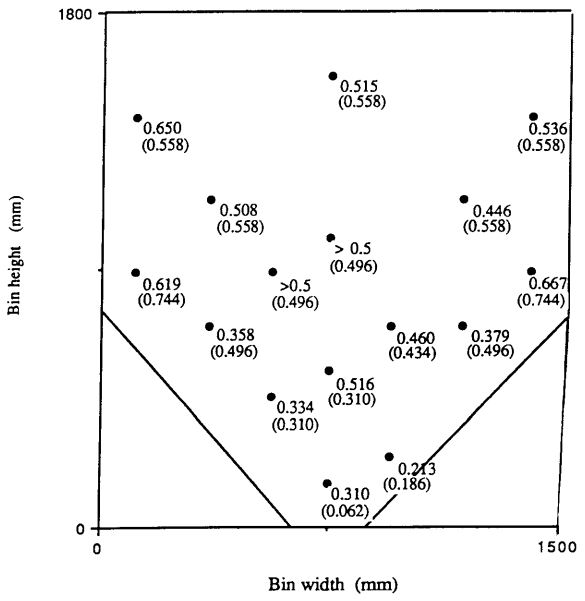

Fig. 7. Measured and simulated (in brackets) air speeds (m/s) in the bin with slanted floor.

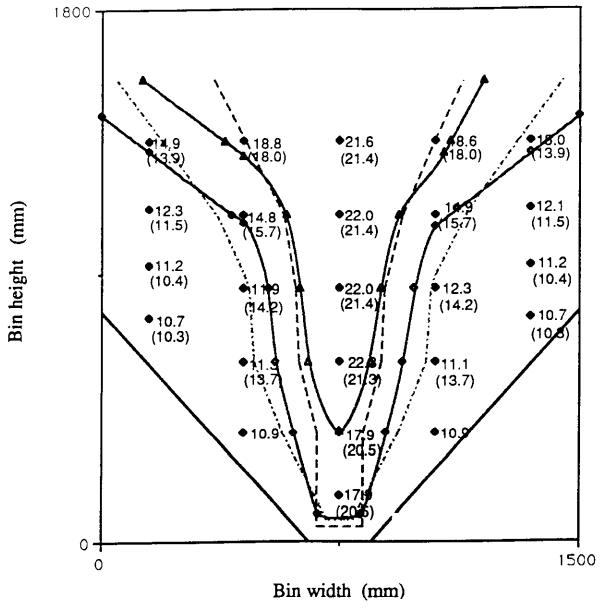

Fig. 8. Measured and simulated (in brackets) moisture contents in the bin with slanted floor. ● 14.5% (Exp.), ▲ 18.0% (Exp.), ····· 14.5% (Sim.), — 18.0% (Sim.).

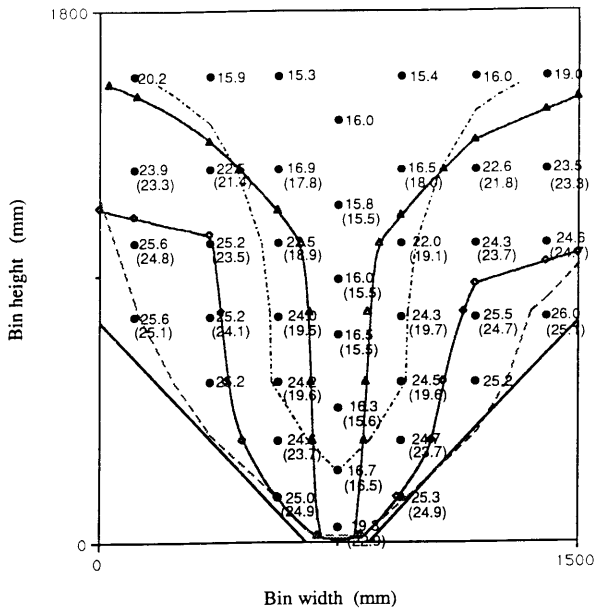

Fig. 9. Measured and simulated (in brackets) temperatures in the bin with slanted floor. $h_v=8.6\times10^8\ [g_a(T+273)/P_{atm}]^{0.6}$. ● 25.0°C (Exp.), △ 20.0°C (Exp.), — 25.0°C (Sim.), ····· 20.0°C (Sim.).

measured value was out of the senor's range. For this bin, the lowest air speed was 0.213 m/s measured at a point near the central bottom of the bin. The measured air speeds increased along the slanted floor. The highest measured air speed was 0.667 m/s at a point close to be more uniform at the upper portion of the bin with partially or slanted perforated floors.

Figure 8 shows the measured and simulated moisture contents. With the slanted floor, a deep core of high moisture content grain was formed due to very low airflow in this area. The core remained wet throughout the drying period. The drying rate in the central part of the bin was slow. Figure 8 shows that the moisture content at the off-center location was 11.1% while the moisture content at the center location, just about 300 mm away from wall, was 22.3% after 65 h of drying.

Figure 9 shows the inter-granular temperatures measured from the tests in bins with slanted perforated floor. The temperatures corresponded to the same time as the moisture contents discussed in the previous section. Two iso temperature lines are plotted. The iso temperature lines in the bin with fully perforated floor were parallel to the bin floor. The temperatures showed some variations at each height, but these variations were within 1°C after 115 h of drying. The shapes of temperature profiles in the bins with partially and slanted perforated floors were similar to the moisture profiles. Temperature distributions in the with partially and slanted perforated floors were not uniform but generally symmetric.

Conclusions

Two major conclusions can be drawn from this research:

1. The orginal drying models based on conservation of mass and energy fail to simulate high temperature drying of grain accurately especially for the grain in a deep bed. A modification of the drying constant for the time and location within the bed improves the performance of the model. The performance of the drying calculations is also enhanced when shrinkage and variable physical properties are accounted for in the model.
2. Airflow into the grain bins depend upon the way air is introduced in the dryer. Conical floors cause a non uniform airflow that could lead to a non uniform temperature and moisture content in the bed. The plug flow assumption for deep bed drying may have to be revised instead true intergranular air velocities are used.

Nomenclatures

〈Symbols〉

a	specific surface area	$m^2 \cdot m^{-3}$
C	specific heat	$J \cdot kg^{-1} \cdot K^{-1}$
f_x	layer factor	
f_t	time factor	
G	permeability	
h	enthalpy	$J \cdot kg^{-1}$
h	convective heat transfer coefficient	$W \cdot m^{-2} \cdot K^{-1}$
hv	volumetric heat transfer coefficient	$W \cdot m^{-3} \cdot K^{-1}$
h_{fg}	heat of vaporization of free water	$J \cdot kg^{-1}$
h'_{fg}	heat of vaporization from the drying product	$J \cdot kg^{-1}$
H	humidity ratio	$kg \cdot kg^{-1}$
g	flow of grain or air	$kg \cdot m^{-2} \cdot s^{-1}$
k	drying constant	s^{-1}
L	bed depth	m
M	moisture content (dry basis)	$kg \cdot kg^{-1}$
n	direction normal	
N	number of layers in drying simulation	
P	pressure	Pa
q	heat transfer rate	$W \cdot m^{-2}$
r	mass exchange rate	$kg \cdot m^{-2} \cdot s^{-1}$
S	shrinkage	fraction
t	time	s
T	temperature	K·°C
v	velocity vector	$m \cdot s^{-1}$
V	air speed	$m \cdot s^{-1}$
x	x-direction, distance	m
y	y-direction, distance	m

〈Subscripts〉

a	air
atm	atmospheric
b	bulk
d	dry
e	exit, equilibrium
i	initial, inlet, direction
m	mass, measured
o	reference point, initial, superficial
p	product
s	dry solid
t	final
v	vapor
w	water
x	distance in x direction

〈Greek〉

ε	porosity

ϕ relative humidity
λ shrinkage
ρ density $kg \cdot m^{-3}$
θ grain temperature
Δt time division
τ drying time factor
Δx distance division
ξ layer factor

Acknowledgments The research reported in this paper was supported financially by Natural Sciences and Engineering Research Council of Canada research grants to S. Sokhansanj.

References

Arthur, J.F. and Rumsey, T.R. (1986). Two-dimensional heat transfer model for packed beds. ASAE Paper No. 86-6003. American Society of Agricultural Engineers, St. Joseph, Michigan, USA.

ASAE STANDARDS (1996). Americans Society of Agricultural Engineers, St. Joseph, Michigan, USA

Bakker-Arkema, F.W., Lerew, L.E. DeBoer, S.F. and Roth, M.G. (1974). Grain dryer simulation. Research Report No. 224. Michigan State University Agricultural Experiments Station, East Lansing, Michigan.

Boyce, D.S. (1965). Grain moisture and temperature changes with position and time during through drying. *J. Agric. Eng. Res.*, **10**, 333–341.

Brooker, D.B. (1959). Computing air pressure and air velocity distribution when air flows through a porous media and non-linear velocity-pressure relationship exist. *Trans. ASAE*, **2**(1), 118–120.

Brooker, D.B. (1961). Pressure patterns in grain-drying system established by numerical methods. *Trans. ASAE*, **4**(1), 72–77.

Brooker, D.B., Bakker-Arkema, F.W. and Hall, C.W. (1974). "Drying Cereal Grain," The AVI Publ. Co., Inc., New York.

Carman, P.C. (1956). "Flow of Gas through Porous Media," Butterworths Scientific Publications, London.

Fasina, O.O. and Sokhansanj, S. (1995). Modeling the bulk cooling of alfalfa pellets. *Drying Technol.* **13**(8 & 9), 1881–1903.

Garrett, R.E. and Brooker, D.B. (1965). Aerodynamic drag of farm grains. *Trans. ASAE,* **8**, 49–52.

Gu, D. (1994). Airflow distribution and its relation to bulk grain drying. Ph.D. Thesis. University of Saskatchewan, Saskatoon, Canada.

Gu, D., Sokhansanj, S. and Norum, D.I. (1996). Intergranular air movement and grain drying in silos with fully, partially, and slanted perforated floor. *Drying Technol.*, **14**(3 & 4), 615–645.

Ingram, G.W. (1976). Deep bed drier simulation with intra-particle moisture diffusion. *J. Agric. Eng. Res.*, **2**, 263–272.

Lam, L. (1990). PC-SEEP Manual. Department of Civil Engineering, University of Saskatchewan, Saskatoon, Canada.

Lang, W., Sokhansanj, S. and Rohani, S. (1994). Dynamic shrinkage and variable parameters in Bakker-Arkema's mathematical simulation of wheat and canola drying. *Drying Technol.*, **12**(7), 1687–1708.

Lang, W. (1993). Drying and wetting of bulk canola and wheat. Ph. D. Thesis. University of Saskatchewan, Saskatoon, Canada.

Li, W.Y. (1992). A generalized model of pressure drop versus airflow for bulk grain. M. Sc. Thesis. University of Saskatchewan, Saskatoon, Canada.

Nishiyama, Y. (1987). Sphere drying model for dryer design. ASAE Paper No. 87-6039. American Society of Agricultural Engineers, St. Joseph, Michigan.

Muir, W.E. and Viravanichai, M. (1972). Specific heat of wheat. *J. Agric. Eng. Res.* **17**, 338–342.

Miketinac, M.J. and Sokhansanj, S. (1985). Velocity-pressure distribution in grain bins—Brooker's mode . *Int. J. Numer. Method Eng.*, **21**, 1067–1075.

O'Callaghan, J.R., Menzies, D.J. and Bailey, P.H. (1971). Digital simulation of agricultural drier performance. *J. Agric. Eng. Res.*, **16**, 223–244.

Segerlind, L.J. (1982). Solving the non-linear airflow equation. ASAE paper No. 823017, American Society of Agricultural Engineers, St. Joseph, Michigan.

Shedd, C.K. (1953). Resistance of grains and seeds to airflow. *Agric. Eng.* **34**, 616–619.

Sokhansanj, S. and Raghavan, G.S. (1996). Drying of grains and forages: a brief review of recent advances. *Drying Technol.*, **14**(6), 1369–1380.